

See discussions, stats, and author profiles for this publication at: <https://www.researchgate.net/publication/228803322>

Mode Tracking of Preselected Vibrations of One-Dimensional Molecular Wires

ARTICLE *in* THE JOURNAL OF PHYSICAL CHEMISTRY A · MARCH 2004

Impact Factor: 2.69 · DOI: 10.1021/jp036825n

CITATIONS

28

READS

17

2 AUTHORS, INCLUDING:



Markus Reiher

ETH Zurich

289 PUBLICATIONS 8,541 CITATIONS

SEE PROFILE

Mode Tracking of Preselected Vibrations of One-Dimensional Molecular Wires

Johannes Neugebauer and Markus Reiher*

Theoretische Chemie, Universität Erlangen-Nürnberg, Egerlandstrasse 3, D-91058 Erlangen, Germany

Received: September 21, 2003; In Final Form: November 21, 2003

The mode-tracking principle (*J. Chem. Phys.* **2003**, *118*, 1634) for the direct quantum chemical calculation of preselected, characteristic molecular vibrations makes vibrational analyses of molecular wire junctions feasible. Characteristic vibrational parameters of molecular bridges such as vibrational frequencies and force constants can be of importance for subsequent treatments in physical model theories of electron transfer and conductance. We investigate how efficient the mode-tracking protocol can be applied to determine such vibrational parameters for a particular type of normal modes of dinuclear polyyne diyl rhenium complexes. The frequencies of vibrations of the carbon chain in complexes of the type $[\text{Re}]-(\text{C}\equiv\text{C})_n-[\text{Re}]$ with $[\text{Re}] = (\eta^5\text{-C}_5\text{Me}_5)\text{Re}(\text{NO})(\text{PPh}_3)$ have been studied as a function of the chain length $2n$, leading to molecules with up to 144 atoms, for which harmonic wavenumbers are determined. The harmonic approximation for the potential-energy surface is compared to explicitly calculated electronic energy values along normal coordinates in order to get an estimate for the role of anharmonicity effects. A possible vibration-induced rupture of molecular bridges is discussed. Different bond-breaking positions for a rupture process in the carbon chain of the rhenium complexes are investigated.

1. Introduction

Molecular bridges and wires currently represent a field of high research activity because of their importance for a bottom-up approach toward mesoscopic electrical devices.^{1–3} The tremendous interest in such molecular electronic building blocks,^{4–6} which might be of use for nanotechnology, also raises new theoretical questions, apart from the experimental ones, which are concerned with problems of synthesis and of tailored physical properties. An intrinsic feature of molecular devices is their mesoscopic length scale. Their range of spatial extension requires different theoretical approaches for the different lengths scales,^{7–9} which cover *first-principles* electronic structure theory as well as simplified molecular mechanical models for interacting atoms or groups of atoms.

The theoretically appealing aspect in the study of mesoscopic devices is that quantum and classical theories meet; Baer and Neuhauser¹⁰ (see also their earlier work)¹¹ proposed a quantum theory for conductance through a molecule clamped between macroscopic electrodes. Their theory is derived for clamped nuclei but it can be extended to include also molecular vibrations. For this extension, the relevant states of the nuclei are needed, and it is the dedicated aim of this work to show how vibrational states can be selectively calculated even for extended systems. Neuhauser et al.¹² studied vibrational coupling and vibrational energy transfer in a one-dimensional lattice, which can serve as a model for a protein or a one-dimensional molecular wire, with three different approaches ranging from *first-principles* quantum mechanics to classical simulations. Their model Hamiltonian was of Toda form and incorporates a Toda potential, which is similar to a Morse potential. In this work, we also point out how such potentials may be efficiently parametrized from *first-principles* calculations by applying

algorithms that allow us to find particular modes of a molecular wire. Once these modes are known, their force constants can easily be used to fit different types of model potentials.

Troisi and Ratner¹⁶ used a model theory to describe the electrical conductance through a molecular rectifier as a function of the applied voltage. The characteristics of the current through the molecule strongly depend on the tendency of the molecule to change conformation upon an applied electrical field, which is modeled in this theory by a parameter (see also ref 17 and references therein for *first-principles* calculations on current-induced conformational changes of molecular wires). A knowledge of the normal coordinates involved in such a conformational change and the corresponding force constants can help to determine parameters for the description of this process. In a recent work¹⁸ by Troisi et al., a rate-constant expression for charge transfer through vibrating bridges is derived, in which the motions of the nuclei also enter. We emphasize that other-than-wire nuclear degrees of freedom of the full system, in particular those of the “electrodes” to which the molecule is attached, are usually neither needed nor wanted; only their electronic effect on the vibrational properties of the molecular junction has to be considered. However, the explicit *first-principles* calculation of the complete many-body nuclear wave function, for which the potential from the electronic structure of an extended composite system were needed, is time consuming if not completely unfeasible. In such situations, a tailored protocol for the calculation of only the important information is needed. While we choose a particular molecular junction described below for our study, we would like to emphasize that the presented methodology is general and of relevance to similar systems.

Both normal modes and vibrational frequencies are ingredients in the study of electron-transfer processes. To give two further examples, we refer the reader to the calculation of electron-transfer rates for which shifts of excited-state structures along the normal modes or reorganization energies are use-

* Author to whom correspondence may be addressed. Theoretische Chemie, Universität Bonn, Wegelerstr. 12, D-53115 Bonn, Germany. Email: Reiher@thch.uni-erlangen.de.

ful.^{14,15} In many studies, the energy gradient of an excited or charge-transfer state with respect to a ground-state normal coordinate is applied in connection with the ground-state vibrational frequency to determine system-specific parameters.¹³

In this work, we set out to apply the recently developed mode-tracking technique.²⁰ With this approach it is possible to reduce the computational costs for a vibrational analyses to the cost of a few electronic structure single-point calculations, i.e., energy and gradient calculations. The calculation of the gradients is usually much faster than the energy calculation. Models of carbon nanotubes²⁰ and the large gold cluster $[(\text{Ph}_3\text{PAu})_6\text{C}]^{2+}$ ²¹ were already successfully analyzed with this novel technique. The mode-tracking approach yields *exact* normal modes and harmonic frequencies for preselected molecular vibrations. The vibrational information accessible by mode-tracking calculations can be used for modeling molecular wires, although this is not explicated here since our focus is on a first analysis of the feasibility of the mode-tracking technique for this purpose.

Since the experimental synthesis of molecular wires is still hampered by a lack of synthetic protocols, which yield reproducible nanoscale wires of well-defined electronic properties, we concentrate in this work on the well-defined systems that were synthesized by Gladysz and co-workers in recent years.²² These examples for molecular wires are stable conjugated hydrocarbons of the polyyne type (i.e., $[-\text{C}\equiv\text{C}-]_n$ chains), which are capped by metal complex fragments and were obtained by well-directed efficient chemical synthesis. These Gladysz-type one-dimensional carbon-chain complexes offer the possibility to conduct electrons through their π system.¹ We study the low-lying motions of the carbon chain in rhenium complexes $[\text{Re}]-(\text{C}\equiv\text{C})_n-[\text{Re}]$ with $[\text{Re}] = (\eta^5\text{-C}_5\text{Me}_5)\text{Re}(\text{NO})-(\text{PPh}_3)$, which were synthesized in the Gladysz group recently;²³ see section 3 for a description of the structures of these complexes. These wavenumbers allow one to draw conclusions on the flexibility of the carbon chain; it is known that the curvature in the solid state for similar Pt compounds can be very different for different chain lengths.²⁴ By a comparison with a simple polyyne chain as a model for the carbon chain in these complexes, one can draw conclusions on the couplings between motions within the chain and motions in the ligands on the rhenium centers in the spirit of a systems theoretical study,^{9,25} which connects properties of analogous (sub)systems in a rigorous manner. Such couplings for an “embedded system” (the chain) in a full cluster can easily be recognized in the mode-tracking approach by the character of the basis vectors that are added in subspace iteration steps (see the following methodology section 2 for details; results are discussed in section 4). In particular, we will study in section 5 how the frequency of the “basic” nodeless vibration of the chain changes as a function of the length of the chain. This may then be used to find simplified models for the estimation of these frequencies for even longer wires. The importance of anharmonicity effects on the tracked vibrations is investigated in section 6. Apart from the vibrational motions of the molecular junction, we also investigate the possibility of a vibrationally induced bridge rupture in Gladysz-type complexes in section 7.

2. Quantum Chemical Methodology

The standard quantum chemical calculation of molecular vibrations in the harmonic approximation²⁶ gets computationally more complicated the more atoms are involved. The reason for this is not the diagonalization of the Hessian matrix, which yields the normal modes, but the computationally very demanding calculation of each of its entries. Since each element requires

the calculation of the second derivative of the electronic energy with respect to coordinates of nuclei in the molecule, the unfortunate scaling behavior of most electronic structure methods (cf., e.g., the discussion in ref 27 but also the new linear-scaling techniques²⁸) for the calculation of the electronic energy is the limiting factor for the vibrational analysis.

Our recently developed mode-tracking approach to molecular vibrations²⁰ circumvents the calculation of the full Hessian matrix *without* introducing any approximation. This is achieved by a combination of the calculation of the second derivatives of the electronic energy (with respect to Cartesian nuclear coordinates and to predefined distortions of these coordinates) and the diagonalization in a subspace iteration method. Since the second derivatives in this procedure are calculated semi-numerically,²⁹ the calculation of preselected, characteristic vibrations is possible for any molecular size for which a structure optimization is possible.

For all density functional theory (DFT) calculations, we used the density-functional programs provided by the TURBOMOLE 5.4 suite.³⁰ All results are obtained from Kohn–Sham-BP86^{31,32} calculations, in which we apply the resolution-of-the-identity (RI) density-fitting technique.^{33,34} Ahlrichs’ SV(P) and TZVP basis sets^{35,36} were employed. For the rhenium atoms, we used the Stuttgart effective core potentials.³⁷

All structures were fully optimized with the corresponding method and basis set. We performed vibrational analyses in a harmonic force field by calculating the second derivatives of the total electronic energy computed as numerical first derivatives²⁹ of analytic energy gradients obtained from TURBOMOLE. The BP86 functional was chosen because it is a reliable functional for the calculation of vibrational frequencies if the calculated harmonic frequencies shall be directly compared to the experimental fundamental ones (i.e., without scaling of frequencies).^{38,39}

For the mode-tracking calculations, we used the AKIRA program.²⁰ The standard quantum chemical method for the calculation of vibrational frequencies and normal modes is to solve the eigenvalue equation

$$(\mathbf{H}^{(m)} - \lambda_k)\mathbf{q}_k = 0 \quad (1)$$

where $\mathbf{H}^{(m)}$ is the mass-weighted Hessian, λ_k is related to the square of the vibrational frequency, and the normal modes are given by the eigenvector \mathbf{q}_k . In the mode-tracking approach, we use a Davidson subspace iteration,⁴⁰ which iteratively leads to the eigenvector \mathbf{q}_k . In iteration step i we solve the approximate eigenvalue problem

$$(\mathbf{H}^{(m)} - \lambda_k^{(i)})\mathbf{q}_k^{(i)} = \mathbf{r}_k^{(i)} \quad (2)$$

where $\lambda_k^{(i)}$ is the i th approximation to the eigenvalue λ_k and the normal mode approximation $\mathbf{q}_k^{(i)}$ is expressed as a sum over basis vectors \mathbf{b}^j ($j = 1, \dots, i$)

$$\mathbf{q}_k^{(i)} = \sum_{j=1}^i C_{j,k} \mathbf{b}^j \quad (3)$$

The coefficients $C_{j,k}$ in this series expansion represent the overlap of the exact normal mode with the basis vectors (N is the number of atoms)

$$C_{j,k} = \langle \mathbf{q}_k | \mathbf{b}^j \rangle = \sum_{i=1}^{3N} q_{k,i} b_i^j \quad (4)$$

These coefficients are calculated “on-the-fly” (see ref 20 for details on the algorithm) since the exact normal mode is only known after convergence. Equation 4 yields the quantitative basis for the systems theoretical analysis;^{9,25} the contribution of the vibrational motion of a well-defined and small local system \mathbf{b}^l to the vibrational motion \mathbf{q}_k of a larger complex, in which the small system is embedded, is given by $C_{1,k}$.

When the residuum vector $\mathbf{r}^{(i)}_k$ for a selected normal mode is sufficiently small, the normal mode approximation is converged to the exact eigenvector \mathbf{q}_k . The exact wavenumber can then be obtained from the corresponding eigenvalue $\lambda^{(i)}_k$.

2.1. Setting up the Local Vibration. As can be seen from eq 2, a guess for the vibrational normal mode is necessary in the first iteration, where $\mathbf{q}_k^{(1)} = \mathbf{b}^l$. Several methods are possible for the construction of normal mode guesses, e.g., results from less expensive quantum chemical calculations or force field models.²⁰ However, semiempirical and empirical calculations require parametrizations, which are not generally available for transition-metal complexes such as those investigated here.

Therefore, we use a different approach here, which additionally offers the possibility to quantify the couplings between an assumed local vibration of a fragment of the complex and the rest of the molecule. First, we partition the full compound in the subsystem that shall be investigated and that which is supposed to constitute the environment. The selected part is usually small enough for a complete harmonic force-field calculation using accurate density functional methods. After the frequency analysis for this subsystem has been performed, one can choose vibrations of interest by inspection of the set of normal modes obtained. These are then employed as a first approximation $\mathbf{q}_k^{(1)}$ for the local vibrations of the subsystem embedded in the full compound.

If the actual vibrations of the embedded subsystem are coupled to the remaining parts of the system, the algorithm will generate new approximations to the true normal mode according to eq 3. The extent of the coupling can be assessed by the magnitude of the coefficients given in eq 4. If the coefficient for the first basis vector $C_{1,k}$ for normal mode k is large, then the assumption of a *local* guess vibration, i.e., one which is essentially localized within the subsystem, is confirmed. Many coefficients of considerable magnitude for a normal mode indicate stronger couplings to the ligands and make the algorithm increase its number of basis vectors step by step.

For the study of the molecular junction, we have chosen the isolated carbon chain as the subsystem and used the mode-tracking protocol to include couplings of this bridge with the vibrations of the rhenium complex fragments through successive iteration steps.

3. Rhenium Complexes with Molecular Bridges of Different Length

We optimized the structures for all complexes of the type $[\text{Re}]-(\text{C}\equiv\text{C})_n-[\text{Re}]$ with $[\text{Re}] = (\eta^5\text{-C}_5\text{Me}_5)\text{Re}(\text{NO})(\text{PPh}_3)$ for values of n from 2 to 10, i.e., 4 to 20 carbon atoms in the chain. We should stress that we have not replaced the $\text{Cp}^* = \text{C}_5\text{Me}_5$ ligands by smaller $\text{Cp} = \text{C}_5\text{H}_5$ ligands. In case of $n = 2$, we also optimized three different diastereomers, which are shown as compounds **1a**, **1b**, and **1c** in Figure 1. The most important structural data are given in Table 1. It can be seen that the bond distances for the three $n = 2$ compounds are quite similar. The largest differences are observed for the $\text{Re}-\text{C}_{\text{cp}}$ distance (up to 0.5 pm). Also the $\text{Re}-\text{Re}$ distance varies by as much as 0.6 pm, but this is negligible compared to the total distance of about 792 pm. The difference of the $\text{Re}-\text{Re}$ distance of 792 pm

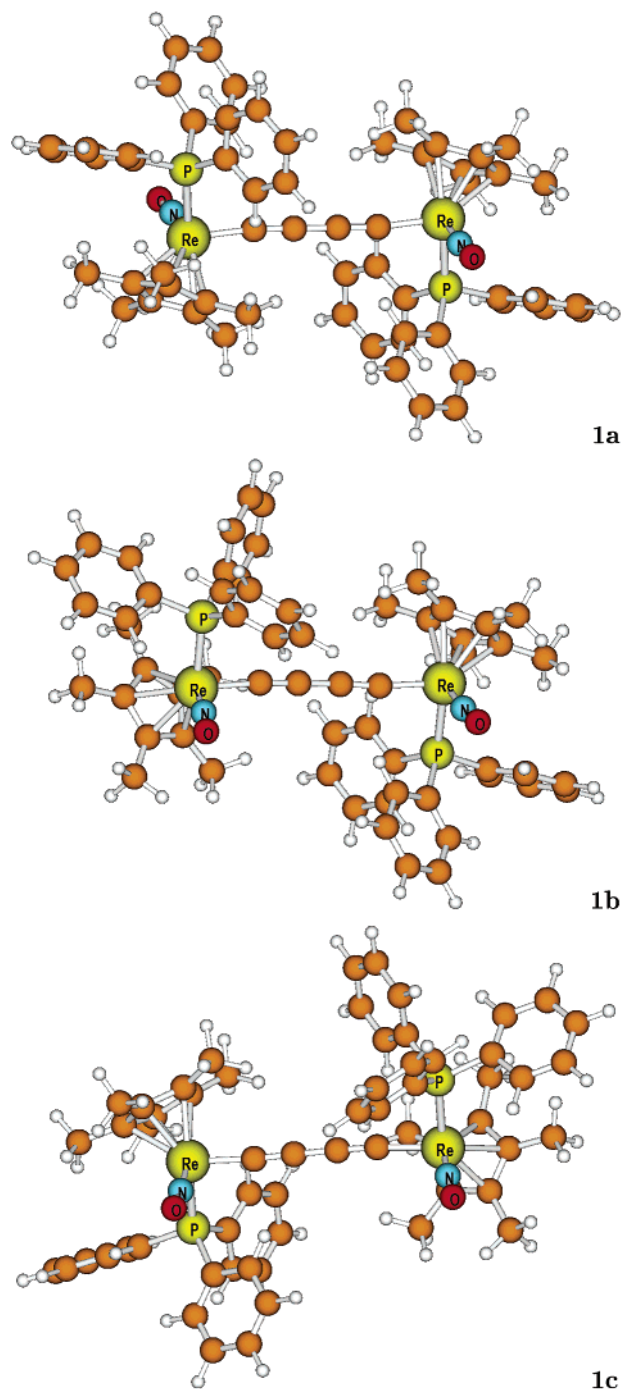


Figure 1. Optimized structures of the diastereomers **1a**, **1b**, and **1c** for the compound $[\text{Re}]-(\text{C}\equiv\text{C})_n-[\text{Re}]$ (shown here are the diastereomers for $n = 2$).

compared to the experimental value of 782.88 pm can easily be explained by summing up the differences in the individual bond lengths.

Even for the largest compounds we find a significant difference in the bond lengths for the $\text{C}\equiv\text{C}$ and the $\text{C}-\text{C}$ bonds, i.e., bond length alternation occurs. The difference between the longer and the shorter bond lengths decreases from 11.0 pm for $n = 2$ to 7.1 pm for $n = 10$. This is in agreement with previous studies on polyyne structures.²³ Also the $\text{Re}-\text{C}_{\text{chain}}$ distance decreases monotonically from 204.2 to 199.4 pm when going from the C_4 to the C_{20} chain. The largest decrease is observed from the C_4 to the C_6 compound (about 3.5 pm), while the chain length decreases by only 2.1 pm from the C_6 to the

TABLE 1: Selected Bond Lengths and Re–Re Distances (Chain Length) of [Re]–(C≡C)_n–[Re] Complexes

<i>n</i>	Re–C _{chain}	(C≡C) _{chain}	(C–C) _{chain}	Re–NO	Re–P	Re–C _{cp}	Re–Re
2a	204.2	124.7	135.7	179.5	242.4	228.7–244.9	792.4
2a, exp 45		120.2(7)	138.9(5)				782.88(4)
2b	204.0	124.8	135.5	179.5	242.3	229.3–244.6	791.8
2c	204.0	124.8	135.5	179.6	242.2	229.2–244.6	791.8
3	201.5	124.8–125.5	133.8	179.7	242.4	230.4–245.0	1044.8
4	201.0	125.1–125.6	132.7–133.4	179.8	243.0	230.7–244.8	1300.9
5	200.6	125.2–125.7	132.3–133.1	179.9	243.3	230.9–244.7	1557.1
6	200.2	125.3–125.8	131.9–132.9	179.9	243.5	231.0–244.6	1813.5
7	200.0	125.4–125.8	131.7–132.8	179.9	243.9	231.3–244.5	2070.4
8	199.7	125.5–125.9	131.5–132.6	180.0	244.0	231.4–244.4	2326.7
9	199.5	125.5–125.9	131.3–132.6	180.0	244.2	231.5–244.4	2583.3
10	199.4	125.6–126.0	131.1–132.5	180.0	244.3	231.7–244.3	2839.8

All values are given in pm. Experimental values are only available for complex 2(a) [45].

C₂₀ chain. As further general trends, we observe that the Re–NO distance becomes slightly larger with increasing chain length, which is also the case for the Re–P bond length and the distance to the carbon atoms in the pentamethyl–cyclopentadienid ligand. The Re–Re distance increases by about 256.1–256.9 pm when adding a C₂ subunit. Only from the *n* = 2–3 compound is the enlargement much smaller (252.4 pm). The estimated Re–Re distance in the Re–C₂₀–Re complex in ref 23 is 28.7 Å, and we obtain a similar value of 28.4 Å. This deviation may be due to slight differences in the individual carbon–carbon and rhenium–carbon bond distances, since no significant bending of the carbon chain is observed in our calculation.

Several studies concerning the electronic structure of these species have been performed over the last years. In ref 23, it is concluded from experimental UV–vis spectra that the HOMO/LUMO energy gap in these complexes is nonvanishing even if the chain length is increased to infinite length. Extrapolation leads to approximately 550 nm for the excitation energy for the first π – π^* excitation. This would also support the observation that there is a considerable bond length alternation for longer carbon chains, while bond-length equalization is usually taken as a hint for vanishing HOMO/LUMO gaps.^{43,44} Bond-length equalization is observed in Hartree–Fock calculations on oxidized systems such as butadiyne²⁺ or related [Re]–C₄–[Re]²⁺ complexes similar to the ones investigated here.⁴⁵ The corresponding HOMOs of the neutral systems were identified to have considerable amplitudes on the metal centers, on the nitrosyl groups, and also partial C₄ π character, so that structural differences between the neutral and the 2-fold cationic forms for the Re–C₄–Re model system are not restricted to the carbon chain. In the above-mentioned work, it was also concluded from NBO analyses that upon 2-fold oxidation 0.74 electrons are lost from the C₄ chain and 0.72 from the nitrosyl ligands. The bonding situation in related [Ru]–C₄–[Ru] complexes was analyzed by extended Hückel and DFT calculations and explained in terms of interactions of frontier molecular orbitals (FMO) in ref 46. The bonding is ascribed to a strong σ -type interaction between high-lying metallic FMOs and low-lying orbitals of the C₄ unit, which leads to an important electron donation toward the metal center. Additionally, a weaker π -type back donation from occupied metallic FMOs to high-lying acceptor C₄ FMOs is recognized. Also for this molecule, it is observed that the HOMO is delocalized over the Ru–C₄–Ru unit, so that electron loss upon oxidation is not purely metal centered. A computational study of odd-numbered carbon chain complexes, which are not investigated here, was conducted by Jiao and Gladysz.⁴⁷

TABLE 2: Vibrational Wavenumbers (BP86/RI/SV(P)) for Selected Normal Modes of the Carbon Chain in Complex 1c from Full Force-Field Calculations Using SNF (Left) and Mode-Tracking Calculations Using AKIRA (Right)^a

no.	SNF	AKIRA
1	117.3	125.1
2	267.7	263.4
3	293.5	291.4

^a The subsystem methodology has been used to obtain initial guesses for the vibrational wavenumbers. All frequencies are given in cm^{–1}.

4. Subsystem Methodology for the Molecular Junction

The Re complexes investigated here are too large to perform systematic vibrational analyses for all compounds using sufficiently large basis sets (up to 144 atoms, corresponding to 2072 contracted Cartesian or 1984 SCF basis functions using the TZVP basis set). As initial guesses in the mode-tracking calculations, we used the subsystem methodology described in section 2.1. We carried out calculations for a polyyne chain of the same length as in the full complex, saturated with hydrogen atoms at the terminating carbon atoms. For these models of the chain, we obtained the complete harmonic force field in a BP86/RI/TZVP calculation with SNF.²⁹ In the calculation of the normal modes, we assigned an artificial mass of 614.16 amu to the two hydrogen atoms. This is the mass of one of the [Re] complex fragments. AKIRA then allows us to use the normal modes for this subsystem as an initial guess for the motions of the Re–C₂₀–Re subunit in the full compound. An initial guess for the Hessian of the full system, which enters the preconditioner in the Davidson algorithm, is not obtained, and a unit matrix is used instead.

In the following, we examine one example for a comparison of a complete force-field calculation from BP86/RI/SV(P) with a mode-tracking calculation using the same method and basis set in order to assess the accuracy of the mode-tracking results. The calculation is carried out for complex 1c, i.e., for a carbon chain with four carbon atoms. As a first test, we used six normal modes obtained in the full force-field calculation as initial guesses for the mode tracking. In all cases, we obtained convergence within one iteration, as one would expect for correct normal modes. The wavenumbers show slight differences of up to 2.5 cm^{–1} in the case of low-frequency modes, while the differences are less than 0.4 cm^{–1} for vibrations in the test set with frequencies > 200 cm^{–1}.

Additionally, we carried out mode-tracking calculations for which we used the subsystem methodology described above. The results for three low-lying vibrations of the carbon chain are given in Table 2. The deviations between the mode-tracking results and the SNF wavenumbers are about 7.8 cm^{–1} for $\tilde{\nu}_1$, 3.3 cm^{–1} for $\tilde{\nu}_2$, and 2.1 cm^{–1} for $\tilde{\nu}_3$. The rather high deviations

TABLE 3: Wavenumbers of the Lowest-Frequency Vibrations of Isolated Carbon Chain Modes of $[\text{Re}]-(\text{C}\equiv\text{C})_n-[\text{Re}]$ Complexes ($\tilde{\nu}$) and the Corresponding Models $\text{H}-\text{C}_x-\text{H}$ ($\tilde{\nu}_{\text{sub}}$) with an Artificial Mass of the Hydrogen Atoms of 614.16 amu^a

n	$\tilde{\nu}_{\text{sub}}$	$\tilde{\nu}$	no. iterations $i + j$
2a	82	120	6 + 5
3	42	77	4 + 3
4	25	53	3 + 8
5	16	45	5 + 4
6	13	44	4 + 5
7	9	40	2 + 7
8	6	29	5 + 7
9	6	32	6 + 2
10	6	32	14 + 3

^a All values are given in cm^{-1} . We also give the number of iterations as $i + j$, where i is the number of initial iterations. From the set of modes produced in these initial iterations, the lowest-frequency mode was chosen and further optimized in a second subspace iteration, which required j iteration steps. Note that in case of $n = 10$ the initial number of iterations is quite large because additional modes (not presented here) have been optimized simultaneously.

for $\tilde{\nu}_1$ and $\tilde{\nu}_2$ demonstrate that the threshold of 0.0005 for $|r_{\text{max}}|$, which was applied here, should be further decreased in order to improve on these results. It should be stressed that the calculations are nontrivial because there are many eigenvalues of the Hessian in the low-frequency range of the rhenium complexes, which may lead to heavy mode-mixing and will thus increase the number of subspace iterations. This is in particular the case for $\tilde{\nu}_1$, which contains large contributions of the other ligands at the rhenium centers, so that many corrections to the initial guess are necessary. Moreover, the relative numerical errors become larger the smaller the vibrational frequencies are, since the energy and gradient changes for a given numerical step size become smaller. This can in principle be overcome by optimizing the step size for a particular normal mode after convergence with the well-chosen default step size has been obtained.

5. Mode Tracking for Modes of the Carbon Chain Attached to the Rhenium Metal Fragments

Since every iteration step introduces numerical errors, it appears advantageous to perform the subspace iteration process in two steps. First, an optimization with a larger threshold (0.0005 for $|r_{\text{max}}|$) is applied, in which several initial guess vectors of low quality are used as basis vectors. After convergence of this calculation, one can select those approximate eigenvectors that are desired in the calculation and start a second mode-tracking calculation with a tighter residuum threshold (0.00025 turned out to be sufficient). This protocol leads to high-quality results for the vibrational wavenumbers and is therefore applied for all calculations in this section. In the first iteration, we optimized at least three low-frequency modes obtained in the subsystem calculation. The lowest frequency of the set of eigenvalues obtained in this calculation was further refined in the second part of the iteration process. The results are given in Table 3 and Figure 2. We also show the vibrational frequencies obtained in the subsystem calculation with SNF (with fictitious masses of 614.16 amu for the hydrogen atoms). The two curves in Figure 2 for the frequencies as a function of the number of carbon atoms in the chain are almost parallel. An exception is the rather small wavenumber obtained for the $n = 8$ compound. But considering the numerical error for these modes of very low frequency, we note that the wavenumbers

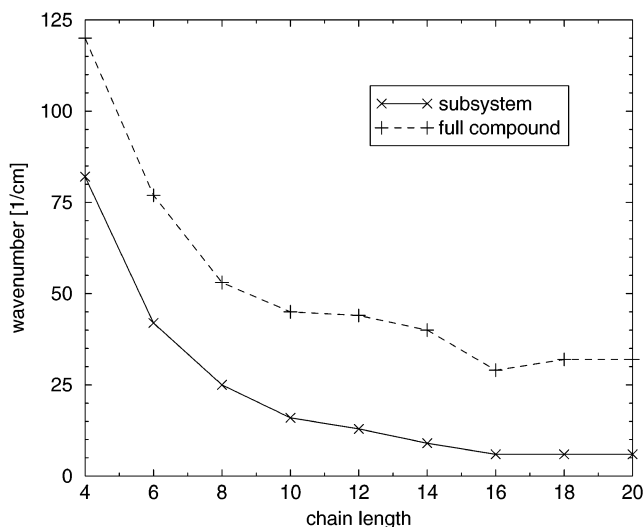


Figure 2. Wavenumbers of the lowest-frequency vibrations of the carbon chain in the compounds of type $[\text{Re}]-\text{C}_x-[\text{Re}]$ as a function of the chain length x (full compound) and of the corresponding models $\text{H}-\text{C}_x-\text{H}$ with an artificial mass of the hydrogen atoms of 614.16 amu. All values are given in units of cm^{-1} .

for the three longest carbon chains of about 30 cm^{-1} are almost equal in the mode-tracking calculation. This is also the case for the subsystem model compound, for which we obtain 6 cm^{-1} for $n = 8, 9$, and 10 .

In case of the $[\text{Re}]-\text{C}_{20}-[\text{Re}]$ complex, we optimized several vibrations of the carbon chain. Three of the vibrations are depicted in Figure 3, which resemble the vibrations of a rope with fixed ends. All vibrations turned out to show nodes at the end of the chain, i.e., at the Re atoms. The first vibration at 32 cm^{-1} has no further nodes and corresponds, thus, to the basic nodeless vibration of a rope, while the second (39 cm^{-1}) and third (56 cm^{-1}) vibrations show one and two additional nodes, respectively, which correspond to the first and second “over-tones” of a rope.

6. Anharmonicity Effects

The motions of the carbon chain investigated in this work are rather “floppy” vibrations with small force constants. For such vibrations, it is important to estimate the effect of anharmonicity of the potential energy surface. Unfortunately, the pure diagonal contribution, i.e., the contribution arising from the third and fourth derivative of the electronic energy with respect to the same normal coordinate to the anharmonic wavenumber correction within vibrational perturbation theory is not well suited to quantify the anharmonicity for that vibration (see, e.g., ref 39). Nonetheless, by studying the potential-energy curve along a normal coordinate, we may get an idea of how important anharmonicity actually is for a given vibration. This knowledge can be useful if model potentials for the corresponding normal mode are employed in subsequent modeling to go beyond that of a pure harmonic oscillator.

We therefore calculated the electronic energy (BP86/RI/TZVP) along the lowest-frequency normal coordinate modes of the carbon chain of the $[\text{Re}]-\text{C}_4-[\text{Re}]$ complex **1a** and of the corresponding model system $\text{H}-\text{C}_4-\text{H}$, which are depicted in Figure 4. The corresponding harmonic approximations to the potential-energy curves according to the harmonic force constants and the zero-point kinetic energy levels are also shown. In the case of the model system $\text{H}-\text{C}_4-\text{H}$, for which again the mass of 614.16 amu was used for the hydrogen atoms, we

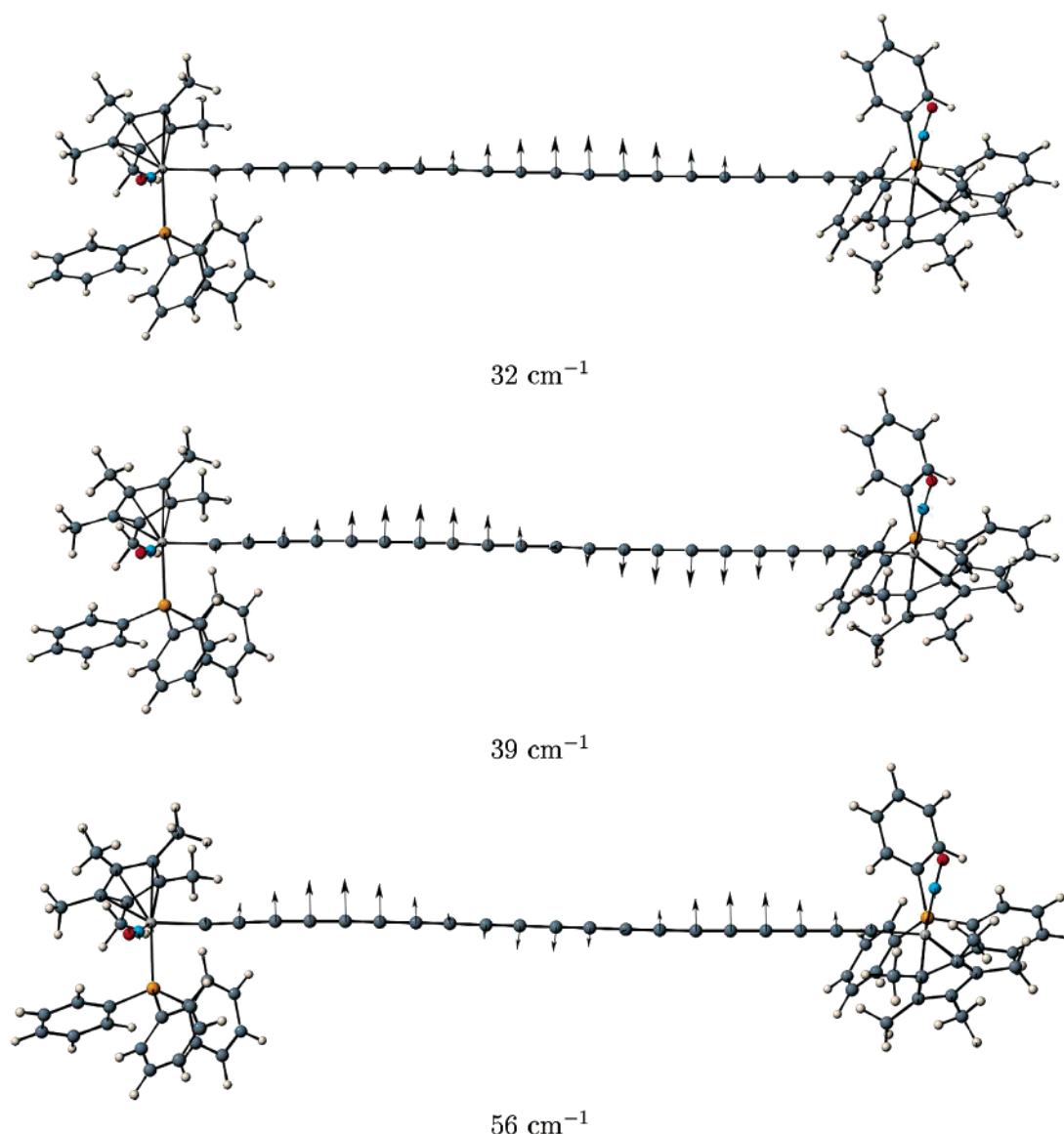


Figure 3. Normal modes and corresponding wavenumbers of the carbon chain in $[\text{Re}]-(\text{C}\equiv\text{C})_{10}-[\text{Re}]$ found via a mode-tracking calculation with AKIRA. The program JMOL [52] was used for the visualization of the normal modes.

observe a remarkably good agreement in the vicinity of the equilibrium structure, while the harmonic approximation is getting slightly worse for larger displacements. For the $[\text{Re}]-\text{C}_4-[\text{Re}]$ complex there are only tiny deviations from the harmonic approximation even near the equilibrium (for ΔQ between 0.5 and 1.0 bohr ($\text{amu}^{1/2}$)), but the relative deviations are smaller for larger displacements along this coordinate, which indicates that the harmonic approximation is better fulfilled for this system. A quadratic fit to the calculated potential-energy curve results in an excellent agreement between the calculated data points and a harmonic potential which corresponds to a wavenumber of 123 cm^{-1} . This is in good agreement with the wavenumber of 120 cm^{-1} calculated with the mode-tracking method. We note that this small deviation stems from the numerical differentiation, which can be improved easily in AKIRA by, e.g., increasing the number of grid points for the discretized derivatives, which also occurs in standard numerical frequency calculations.

From the calculations reported in this section, we conclude that anharmonicity effects play a minor role in molecular junctions, which are symmetrically attached to two heavy

anchors, even if the vibration is a low-frequency bending motion of the whole bridge.

7. Rupture of the Molecular Bridge

The results from the frequency analyses exhibit many low-frequency vibrations of the carbon chain, which are already excited at room temperature, particularly in the case of the longer chains. To study the possibility of rupture processes of the molecular bridge in these complexes, we calculated BP86/RI/TZVP energies for the breaking of the chain $[\text{Re}]-\text{C}_{20}-[\text{Re}]$ into two fragments. Decompositions into fragments ($[\text{Re}]$, $\text{C}_{20}-[\text{Re}]$), ($[\text{Re}]-\text{C}_2$, $\text{C}_{18}-[\text{Re}]$), and ($[\text{Re}]-\text{C}_{10}$, $\text{C}_{10}-[\text{Re}]$) were taken into account, where we considered neutral as well as charged fragments. The reaction energies in Table 4 show that none of the breaking processes is energetically favorable. The products are in all cases less stable than the reactant. (There is no need for a counterpoise correction of the data because of the magnitude of the energy values). Even structural relaxation of the fragments, for which we give the energetics in the lower half of Table 4, does not lead to a substantial lowering of the reaction energies. Two conclusions can be drawn from the

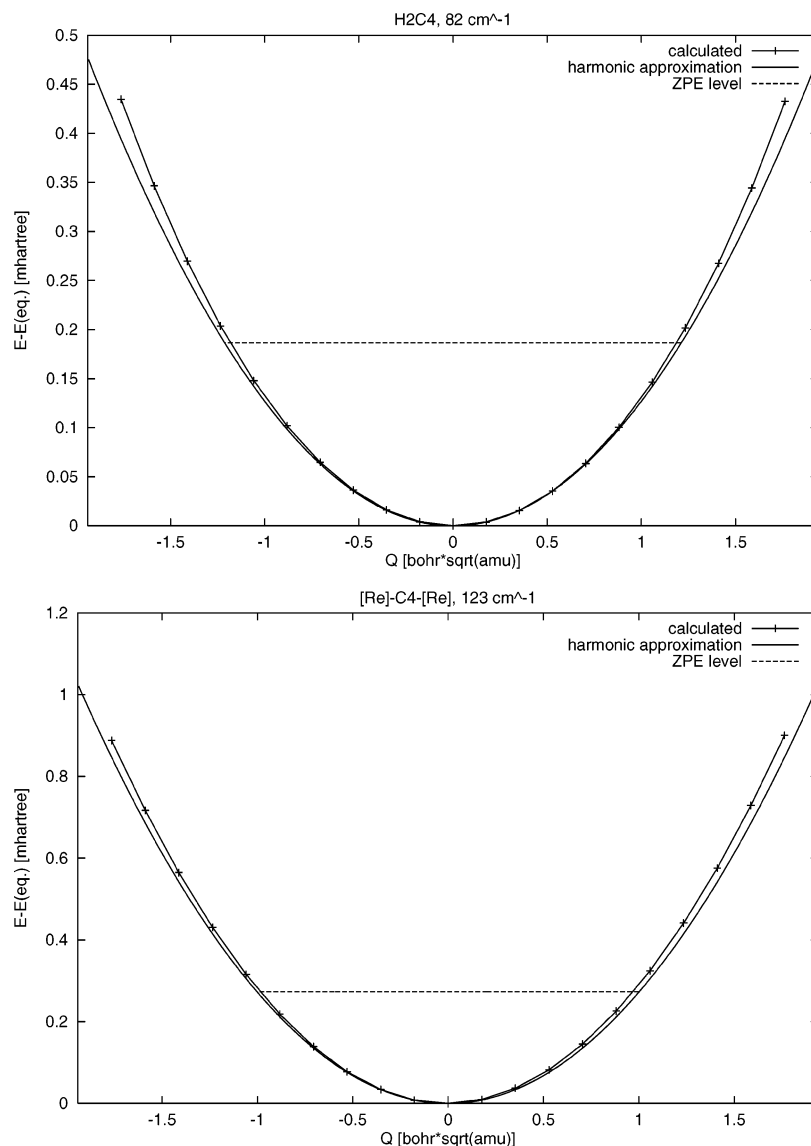


Figure 4. Potential energy curves along the lowest-frequency vibrational normal coordinate for a motion of the carbon chain of the $[\text{Re}]\text{--C}_4\text{--}[\text{Re}]$ complex **1a** (bottom) and the corresponding model system $\text{H--C}_4\text{--H}$ (top) with artificial masses of 614.16 amu for the hydrogen atoms, calculated using BP86/RI/TZVP. Also shown are the harmonic approximations for the potential energy along these normal coordinates and the zero-point kinetic energy levels as well as the wavenumbers in cm^{-1} from a quadratic fit to the data points.

results. First, the breaking into two neutral fragments is for all rupture positions more favorable than a decomposition into charged fragments, which might change if solvent effects are considered. Second, among these decomposition processes, the bond breaking at one of the two metal centers is energetically preferred compared to bond breakings within the carbon chain. Our results are in line with the experimental facts²³ that these metal-capped, wirelike polyynediyl chains are remarkably stable in the solid state and thermally decompose only at temperatures above 150 °C, which is ascribed to chain–chain cross linking. A possible reason for the lability of $[\text{Re}]\text{--C}_{20}\text{--}[\text{Re}]$ in solution are similar impurity-catalyzed cross-linking mechanisms.

On a mesoscopic length scale, forces other than those induced by collisions in chemical reactions can become important, for which the energetical analysis presented in this section will be valuable. Theoretical investigations into mechanically induced processes have been conducted by Marx and collaborators⁴⁸ for organic molecules attached to gold clusters and by Frank et al.^{49–51} The latter authors also derived a simple model with system-specific and thermodynamic parameters (bond type, pulling rate, temperature) in order to predict the bond-breaking

TABLE 4: Reaction Energies ΔE_{rupt} in kJ/mol for the Rupture of the Carbon Bridge in $[\text{Re}]\text{--C}_{20}\text{--}[\text{Re}]$ into Neutral, Anionic, and Cationic Fragments $[\text{Re}]\text{--C}_n$ and $\text{C}_m\text{--}[\text{Re}]$, Obtained from BP86/RI/TZVP Calculations

n	m	ΔE_{rupt}
Unrelaxed		
0 (anion)	20 (cation)	958
0 (cation)	20 (anion)	595
0 (neutral)	20 (neutral)	435
10 (anion)	10 (cation)	876
10 (cation)	10 (anion)	876
10 (neutral)	10 (neutral)	542
2 (anion)	18 (cation)	1008
2 (cation)	18 (anion)	836
2 (neutral)	18 (neutral)	563
Relaxed		
0 (anion)	20 (cation)	858
0 (cation)	20 (anion)	567
0 (neutral)	20 (neutral)	408
10 (anion)	10 (cation)	844
10 (cation)	10 (anion)	844
10 (neutral)	10 (neutral)	533
2 (anion)	18 (cation)	953
2 (cation)	18 (anion)	790
2 (neutral)	18 (neutral)	546

probability. The model involves simple springs for each bond. The results obtained in this work would allow one to use a more elaborate spring model for the collective motions of the ropelike wire in such approaches. It is noteworthy that Röhrig and Frank⁴⁹ also find in their *first-principles* molecular dynamics calculations a polymer breaking at its attachment positions on a surface.

8. Conclusion

The mode-tracking calculations show that the “out-of-line” vibrations of the carbon chain in Gladysz-type rhenium complexes are of very low frequency. The wavenumber for the lowest-frequency vibration, which corresponds to the basic nodeless vibration of a rope as a model for the carbon chain, steadily decreases with increasing chain length, until a saturation is reached for about 16 carbon atoms in the chain. This suggests that bending of the carbon chain and deformations might easily be possible and also explains the curvatures of analogous compounds found in the solid state by X-ray analysis,²⁴ where packing effects can become important. The vibrational frequencies obtained here can further be used to develop a model for the vibrational frequencies of molecular wires as a function of the chain length. This would permit us to give estimates of the vibrational frequencies for even longer one-dimensional wires.

The sample complexes studied in this work demonstrate how the mode-tracking algorithm can be efficiently applied for the calculation of nonlocal vibrations, which couple motions of all atoms of the subsystem (without using an appropriate initial guess for the preconditioner). The computational effort was largely reduced. The calculation for [Re]–C₁₈–[Re], for instance, required eight iterations in total, in which 10 basis vectors were employed. Three basis vectors were converged according to the less tight convergence criterion in the first part of the subspace iteration, one of which was further refined in the second part. This means that three vibrational frequencies are obtained from 20 single-point calculations (energy plus gradient). By contrast, the complete Hessian is of dimension 426×426 and would require 852 single-point calculations.

The convergence behavior was slightly worse in case of the shortest carbon chains, in particular for the $n = 2$ compound. This is, however, no drawback of the algorithm but a consequence of the stronger couplings with the metal complex fragments. The stronger the couplings, the more additional basis vectors are necessary to take motions of the other ligands at the rhenium atoms into account. In case of longer carbon chains, however, these couplings are less important, and additional basis vectors are necessary to improve the description of the motions within the chain.

It should be emphasized that it is easy to use mode tracking also for other types of vibrations. During the first iteration steps, for example, we also obtained estimates for various carbon–carbon stretching vibrations in the chain, which we did, however, not choose for refinement in subsequent calculations. Furthermore, it is straightforward to calculate certain properties with respect to these normal modes, once they are known from a mode-tracking calculation. Examples are forces in excited states along these modes, which can be obtained by two calculations of excitation energies for structures displaced along the normal coordinate. Therefore, this approach should provide the means to efficiently calculate the data necessary for the parametrization of certain model theories related to electron transfer and molecular conductance.

The general result in this work for molecular devices and especially for molecular wires is the demonstration of feasibility

and reliability of *first-principles* quantum chemical methods to provide system-specific information useful for more approximate models. Consequently, tailored quantum chemical protocols such as the mode-tracking approach close the gap between explicit and accurate quantum chemical methods and model theories based on quantum mechanics or molecular mechanics.

Acknowledgment. This work was supported by the Deutsche Forschungsgemeinschaft DFG in the framework of the collaborative research center SFB 583 and by the Fonds der Chemischen Industrie (FCI). J.N. gratefully acknowledges funding by a Kekulé-Stipendium of the FCI.

References and Notes

- (1) Robertson, N.; McGowan, C. A. *Chem. Soc. Rev.* **2003**, 32, 96–103.
- (2) Nitzan, A.; Ratner, M. A. *Science* **2003**, 300, 1384–1389.
- (3) Metzger, R. M. *Chem. Rev.* **2003**, 103, 3803–3834.
- (4) Datta, S. *Electronic Transport in Mesoscopic Systems*; Cambridge University Press: Cambridge, 1995.
- (5) Jortner, J.; Ratner, M. *Molecular Electronics*; Blackwell Science: Oxford, 1997.
- (6) Aviram, A.; Ratner, M. A. *Molecular Electronics: Science and Technology*; New York Academy of Sciences: New York, 1998.
- (7) Kremer, K.; Müller-Plathe, F. *MRS Bull.* **2001**, 205–210.
- (8) Müller-Plathe, F. *Chem. Phys. Chem.* **2002**, 3, 754–769.
- (9) Reiher, M. *Found. Chem.* **2003**, 5, 23–41.
- (10) Baer, R.; Neuhauser, D. *Chem. Phys. Lett.* **2003**, 374, 459–463.
- (11) Baer, R.; Neuhauser, D. *Int. J. Quantum Chem.* **2003**, 91, 524–532.
- (12) Neuhauser, D.; Baer, R.; Kosloff, R. *J. Chem. Phys.* **2003**, 118, 5729–5735.
- (13) Myers, B. A. *Chem. Rev.* **1996**, 96, 519–527.
- (14) Hupp, J. T.; Williams, R. D. *Acc. Chem. Res.* **2001**, 34, 808–817.
- (15) Biswas, N.; Umapathy, S. *J. Chem. Phys.* **2003**, 118, 5526–5536.
- (16) Troisi, A.; Ratner, M. A. *J. Am. Chem. Soc.* **2002**, 124, 14528–14529.
- (17) Ventra, M. D.; Pantelides, S. T.; Lang, N. D. *Phys. Rev. Lett.* **2002**, 88, 046801.
- (18) Troisi, A.; Nitzan, A.; Ratner, M. A. *J. Chem. Phys.* **2003**, 119, 5782–5788.
- (19) Xu, B.; Tao, N. J. *Science* **2003**, 301, 1221–1223.
- (20) Reiher, M.; Neugebauer, J. *J. Chem. Phys.* **2003**, 118, 1634–1641.
- (21) Neugebauer, J.; Reiher, M. *J. Comput. Chem.* **2004**, 25, 587–597.
- (22) Szafert, S.; Gladysz, J. A. *Chem. Rev.* **2003**, 103, 4175–4205.
- (23) Dembinski, R.; Bartik, T.; Bartik, B.; Jaeger, M.; Gladysz, J. A. *J. Am. Chem. Soc.* **2000**, 122, 810–822.
- (24) Mohr, W.; Stahl, J.; Hampel, F.; Gladysz, J. A. *Inorg. Chem.* **2001**, 40, 3263–3264.
- (25) Reiher, M. *Found. Chem.* **2003**, 5, 147–163.
- (26) Wilson, E. B.; Decius, J. C.; Cross, P. C. *Molecular Vibrations*; McGraw-Hill: New York, 1955.
- (27) Helgaker, T.; Jørgensen, P.; Olsen, J. *Molecular Electronic-Structure Theory*; Wiley: New York, 2000.
- (28) Goedecker, S. *Rev. Mod. Phys.* **1999**, 71, 1085–1123.
- (29) Neugebauer, J.; Reiher, M.; Kind, C.; Hess, B. A. *J. Comput. Chem.* **2002**, 23, 895–910.
- (30) Ahlrichs, R.; Bär, M.; Häser, M.; Horn, H.; Kölmel, C. *Chem. Phys. Lett.* **1989**, 162, 165–169.
- (31) Becke, A. D. *Phys. Rev. A* **1988**, 38, 3098–3100.
- (32) Perdew, J. P. *Phys. Rev. B* **1986**, 33, 8822–8824.
- (33) Eichkorn, K.; Treutler, O.; Öhm, H.; Häser, M.; Ahlrichs, R. *Chem. Phys. Lett.* **1995**, 240, 283–290.
- (34) Eichkorn, K.; Weigend, F.; Treutler, O.; Ahlrichs, R. *Theor. Chem. Acc.* **1997**, 97, 119–124.
- (35) Schäfer, A.; Horn, H.; Ahlrichs, R. *J. Chem. Phys.* **1992**, 97, 2571.
- (36) Schäfer, A.; Huber, C.; Ahlrichs, R. *J. Chem. Phys.* **1994**, 100, 5829.
- (37) Andrae, D.; Häussermann, U.; Dolg, M.; Stoll, H.; Preuss, H. *Theor. Chim. Acta* **1990**, 77, 123.
- (38) Reiher, M.; Neugebauer, J.; Hess, B. A. *Z. Physik. Chem.* **2003**, 217, 91–103.
- (39) Neugebauer, J.; Hess, B. A. *J. Chem. Phys.* **2003**, 118, 7215–7225.
- (40) Davidson, E. R. *J. Comput. Phys.* **1975**, 17, 87–94.
- (41) Stewart, J. J. P. *Quantum Chem. Prog. Exch.* **1990**, 10, 86.

- (42) Serena Software, "PCMODEL", <http://www.serenasoft.com/pcm8.html>, 2003.
- (43) Hoffmann, R. *Angew. Chem.* **1987**, 99, 871–906.
- (44) Hoffmann, R. *Angew. Chem., Int. Ed. Engl.* **1987**, 26, 846.
- (45) Brady, M.; Weng, W.; Zhou, Y.; Seyler, J. W.; Amoroso, A. J.; Arif, A. M.; Böhme, M.; Frenking, G.; Gladysz, J. A. *J. Am. Chem. Soc.* **1997**, 119, 775–788.
- (46) Bruce, M. I.; Low, P. J.; Costuas, K.; Halet, J.-F.; Best, S. P.; Heath, G. A. *J. Am. Chem. Soc.* **2000**, 122, 1949–1962.
- (47) Jiao, H.; Gladysz, J. A. *New J. Chem.* **2001**, 551–562.
- (48) Krüger, D.; Fuchs, H.; Rousseau, R.; Marx, D.; Parrinello, M. *Phys. Rev. Lett.* **2002**, 89, 186402.
- (49) Röhrig, U. F.; Frank, I. *J. Chem. Phys.* **2001**, 115, 8670–8674.
- (50) Aktah, D.; Frank, I. *J. Am. Chem. Soc.* **2002**, 124, 3402–3406.
- (51) Röhrig, U. F.; Troppmann, U.; Frank, I. *Chem. Phys.* **2003**, 289, 381–388.
- (52) The Jmol team, "Jmol", <http://jmol.sourceforge.net>, 2003.
- (53) National Institute of Standards and Technology, "NIST Chemistry WebBook", <http://webbook.nist.gov/>, 2003.